J Mol Model (2012) 18:2493–2500
DOI 10.1007/s00894-011-1269-z

ORIGINAL PAPER

Role of cationic size in the optical properties of the LiCl crystal surface: theoretical study

Wael Salah Abdel Halim · Noha Abdullah · Safaa Abdel-Aal · A. S. Shalabi

Received: 10 June 2011 / Accepted: 4 October 2011 / Published online: 28 October 2011

Abstract The size of the cations (either Ca^{2+}, Sr^{2+}, Ga^{+}, or Au^{+}) at the F_{A1}-type color centers on the (100) surface of LiCl crystal plays an important role in the optical properties of this surface. In this work, double-well potentials at this surface were investigated using ab initio quantum mechanical methods. Quantum clusters were embedded in simulated Coulomb fields that closely approximate the Madelung fields of the host surface, and the ions that were the nearest neighbors to the F_{A1} site were allowed to relax to equilibrium. The calculated Stokes-shifted optical transition bands, optical–optical conversion efficiency, and relaxed excited states of the defect-containing surface, as well as the orientational destruction of the color centers, recording sensitivity, exciton (energy) transfer, and the Glasner–Tompkins empirical relation were all found to be sensitive to the size of the dopant cation.

Keywords Optical properties · LiCl surface · F_{A1}:Ca^{2+} · F_{A1}:Sr^{2+} · F_{A1}:Ga^{+} · F_{A1}:Au^{+}

Introduction

The modeling of solid-state processes has reached the stage at which it can be usefully employed for applications in solid-state chemistry and physics. Theoretical modeling is an especially powerful tool when searching for new materials, as it can narrow down the list of potential materials for which crystal growth techniques need to be developed. The application of theoretical models would provide benefits when testing laser light generation. There have been a few detailed theoretical studies of the key processes associated with color center lasers. Such studies can suggest paths to new systems or to improvements in existing systems.

In the work described in the present paper, we considered how the size of the cations at some selected color centers on the regular surface of LiCl crystal influences the luminescence activities of such color centers. Aside from the data for the F_{A1}:Sr^{2+} color center reported by Abdel Aal [1], neither theoretical nor experimental data are currently available for the F_{A1}-type color centers present on the surface of LiCl. However, experimental investigations have been carried out for Sr-doped NaCl crystal by Joshi and Kekan [2] and the polycrystalline ceramic Sr_2FeMoO_6 by Greneche et al. [3].

An F center consists of an anion vacancy binding an electron, while the more complex F_A center is an F center attached to a cationic impurity. In F_A centers [4], the threefold-degenerate $2p$ state of the F center is split during absorption due to the adjacent cationic impurity, thus forming two well-resolved absorption bands, F_{A1} and F_{A2}. Two types of centers can therefore be distinguished, corresponding to the different relaxation behaviors of the centers after optical excitation. In type F_{A1} centers, the F center is attached to a large cationic impurity; in type F_{A2} centers, the F center is attached to a small cationic impurity relative to the host cation.

As far as laser light generation is concerned, electron–phonon coupling causes broadened Stokes-shifted optical transition bands. The electrons associated with a defect interact strongly with the surrounding vibrating crystal ions,

W. S. Abdel Halim · N. Abdullah
Department of Chemistry, Faculty of Science, Zagazig University, P.O. Box 44519, Zagazig, Egypt

S. Abdel-Aal · A. S. Shalabi (✉)
Department of Chemistry, Faculty of Science, Benha University, P.O. Box 13518, Benha, Egypt
e-mail: asshalabi@hotmail.com

resulting in optical transitions, which are allowed in a broad band around the defect-specific central transitions. All of the color center lasers realized so far are based on electronic defects. In 1991, Gellerman [5–8] reviewed some of the optical and laser properties of the most important examples of color center species in alkali halide crystals, and reported that color centers in these crystals can be applied as high-gain active materials in tunable solid-state lasers. Using various color center types and host lattices, the combined tuning range of color center lasers covers the near-infrared region from about 0.8 to 4 μm.

The possible energy level structure for the electron at an F_A center is influenced by the shape and depth of the electronic binding potential. This potential is determined mainly by the distance and geometrical arrangement of the nearest surrounding lattice ions, which oscillate around their equilibrium positions. Therefore, the potential changes dynamically with the vibrations of the ions. This in turn modifies the electronic energy levels and charge distributions. The ionic equilibrium varies with the electronic state, and the electron–phonon coupling and its effect on the optical transitions can be illustrated using a configuration coordinate diagram [9].

The development of color center lasers depends on investigations of known color center systems with more favorable optical properties as well as the development of new laser-active defects. It appears that a laser-suitable defect should have the following properties: (1) one electron defect center, (2) compact electronic states, (3) relaxed excited states deep below the conduction band, and (4) it should be possible to experimentally produce such centers in high concentrations ($\geq 5\times10^{16}$ cm^{-3}) [10].

Ab initio calculations of laser light generation at the ionic crystal surface are still lacking, and until recently the potential of F_{A1}:Ga^+, Au^+, and Ca^{2+} center systems to supply useful laser action at the (100) surface of LiCl has been ignored [11–13]. We have therefore carried out a fairly extensive set of ab initio calculations in an attempt to examine the role of cationic radii of the doping cations Ga^+, Au^+, Ca^{2+}, and Sr^{2+} in laser light generation at the (100) surface of LiCl. Several related optical properties were also considered.

We have not been able to find any experimental data on the characteristics of laser light generation by the color centers of interest at the LiCl surface. Hence, our results serve as theoretical predictions.

The present study is organized as follows. "Methods" gives a brief account of the theoretical methods, namely, simulation of the low coordination (100) surface of LiCl, configuration interaction singles (CI singles), and configuration coordinate diagrams (CC diagrams). In "Results and discussion," the results for laser light generation by the double-well potentials of the F_{A1}:Ga^+, Au^+, Ca^{2+}, and Sr^{2+} color centers are given and discussed. The results are then summarized and conclusions are drawn.

Methods

Crystal simulation

There are several methods that can be employed to simulate crystals, using either finite or infinite systems [14–19]. In the case of finite systems, only local portions of the crystal are considered. For such an approach, clusters of varying sizes in the bulk structure are suitable approximations. In the present study, we used a finite system to simulate the LiCl crystal.

Bulk simulation

A finite ionic crystal with 288 point charges was first constructed. The Coulomb potentials along the *X* and *Y* axes of this crystal were zero due to the symmetry of the host crystal. The ±1 charges on the outer shells were then modified, using a fitting procedure, to make the Coulomb potential at the four central sites closely approximate the Madelung potential of the host crystal, and to make the Coulomb potential at the eight points with coordinates (0, ±*R*, ±*R*) and (±*R*, 0, ±*R*), where *R* is half the lattice distance (which for LiCl is 2.57 Å), equal to zero, as it is in the host crystal. When the resulting charges (0.409283 and 0.800909) are used, the Coulomb potential in the region occupied by the central ions is very close to that in the unit cell of the host crystal. The Coulomb potential was calculated to be 1.748 at the four central sites (compared with 1.746 for a simple cubic ionic crystal) and 0.0 at the previously defined eight points (compared with 0.0 for the same crystal).

Surface simulation

All charged centers with Cartesian coordinates (±*X*, ±*Y*, $Z>0$) were eliminated to generate the (100) surface of LiCl, with 176 charged centers occupying the three-dimensional space (±*X*, ±*Y*, $Z\leq0$). The clusters shown in Fig. 1 were then embedded within the central region of the crystal surface. All of the electrons of the embedded clusters were included in the Hamiltonians of the ab initio calculations. Other crystal sites entered the Hamiltonians as either full or partial ionic charges.

To account for the significant chemical effects associated with the creation of the defect, the clusters adopted to describe the F_{A1}:Ga^+, Au^+, Ca^{2+}, and Sr^{2+} color centers that generate laser light at the LiCl surface were denominated [$Li_8Cl_{13}F_{A1}$] (Fig. 1).

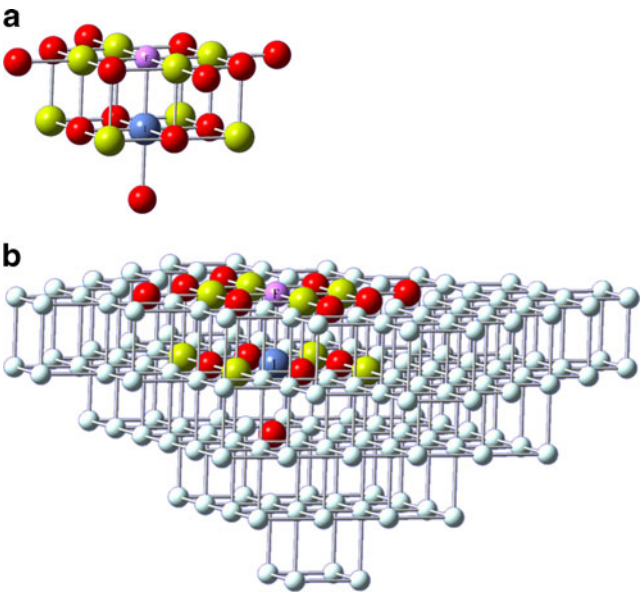

Fig. 1 **a** Representative sketch of the surface clusters considered in the calculations. *Red* Cl^-, *yellow* Li^+, *pink (F)* F center, *blue (I)* impurity cation. **b** Representative sketch of the surface clusters embedded in point charges. *Red* Cl^-, *yellow* Li^+, *pink (F)* F center, *blue (I)* impurity cation

Calculations

Configuration coordinate diagrams

The geometric relaxation of F_A centers in the ground and excited states is key to laser activity due to vibronic coupling. In other words, the possible energy level structure of the F_A center electron is influenced by the shape and depth of the electronic binding potential. This potential is determined mainly by the geometrical arrangement of the nearest surrounding lattice ions, which oscillate around their equilibrium positions. The ionic equilibrium varies with the electronic state, and the electron–phonon coupling and its effect on the optical transitions can be illustrated using the well-known configuration coordinate diagram [20]. In the configuration coordinate diagram, the electronic energies in the ground and excited states are plotted versus the configuration coordinate Q, which represents a certain localized or normal mode of the lattice coupling to the electron. In other words, Q represents the simultaneous displacement of the cations that are the nearest neighbors to the defect site from the lattice interionic separation (Q=0.0) along the axes joining them with the defect site. This is called the symmetric (or linear) coupling mode. The other ions were retained at their original positions in the lattice. Starting from the ground state of the F_A center, an optical excitation produces a transition into the excited state at fixed nuclear coordinates assuming the Franck–Condon principle (i.e., vertical transitions in the configuration coordinate diagram). Due to the Gaussian-shaped probability function for the lowest vibrational state, the transition most probably starts from the equilibrium position Q_1. The electronic distribution reached immediately after excitation is not in equilibrium with the lattice at Q_1. As a consequence, the ions oscillate toward a new equilibrium position. The vibrational energy will be dissipated via anharmonicity into lattice phonons, and the lattice will reach the new equilibrium position Q_2, i.e., the relaxed excited state. After the mean lifetime has elapsed, the excited electron returns by a vertical emission process to the ground state, and the subsequent lattice relaxation completes the optical cycle [5–8]. To construct the configuration coordinate diagrams, the ion clusters representing the F_{A1}:Ga^+, F_{A1}:Au^+, F_{A1}:Ca^{2+}, and F_{A1}:Sr^{2+} centers on the (100) surfaces of LiCl were first embedded into the three-dimensional arrays of the point ions described in the "Surface simulation" section. The representations of the ion clusters are given in Fig. 1. The absorption and emission energies were then calculated as the difference between the total energies of the ground and excited states. To achieve this, the relevant potential energy curves were calculated, and then—according to the Franck–Condon principle—the absorption energy was calculated as that for a vertical transition from the minimum of the relaxed ground state to the excited state. The luminescence energy was calculated in a similar manner. Stokes shifts were then calculated as the difference between absorption and emission energies:

$$\Delta E_{\text{absorption}} - \Delta E_{\text{emission}}.$$

Table 1 The minima for the ground states (Q_1) and low-lying excited states (Q_2), horizontal shifts along the configuration coordinate ($Q_2 - Q_1$), and absorbed and emission transition energies ΔE between the ground electronic states (g) and the low-lying excited electronic states (e) of F^+_A centers at the (100) surface of LiCl crystal, calculated at the CIS level. R=1.285 Å, and energies are in eV

Crystal	Impurity	Q_1/R	Q_2/R	$(Q_2 - Q_1)$	$\Delta E_{\text{absorption}}$	$\Delta E_{\text{emission}}$	Stokes shift
LiCl	Ga^+	2.518	2.886	0.368	1.9368	0.7787	1.1581
	Au^+	2.625	2.881	0.256	1.9742	1.146	0.8282
	Ca^{2+}	2.758	2.985	0.227	3.1459	1.9713	1.1746
	Sr^{2+} [a]	2.672	2.896	0.224	3.3631	2.4914	0.8717

[a] Reproducible data that were identical to those in [1]

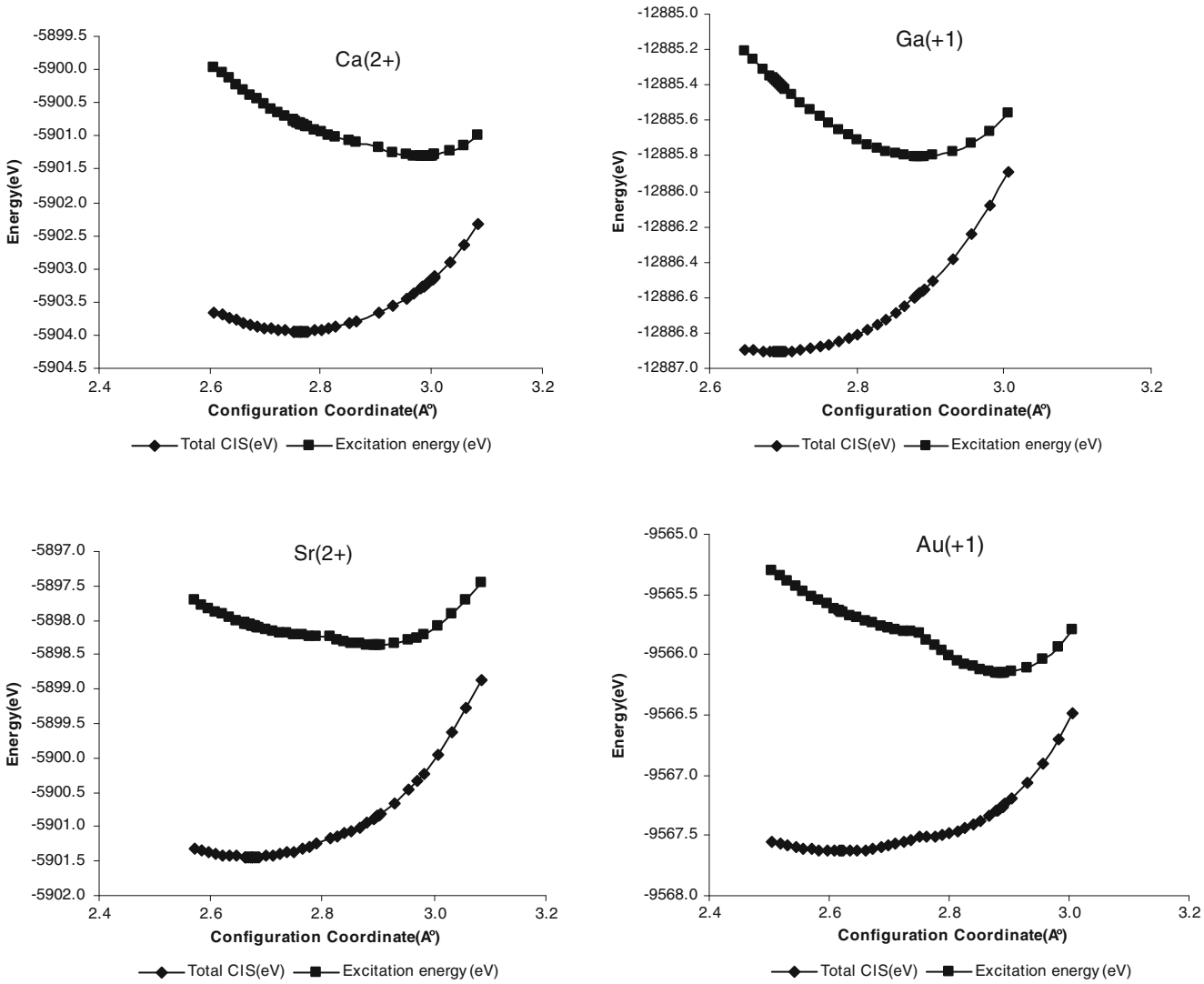

Fig. 2 Configuration coordinate diagrams for the F_{A1}:Ga^{+}, F_{A1}:Au^{+}, F_{A1}:Ca^{2+}, and F_{A1}:Sr^{2+} laser color centers on the (100) surface of LiCl

Configuration interaction singles method

The configuration interaction singles method was employed to calculate the F_A laser activity, the relaxed excited state orientational destruction of the F_A center, and the reorientational efficiency. The configuration interaction singles method uses the configuration interaction approach and models excited states as combinations of single substitutions out of the Hartree–Fock ground state. The CI singles theory is an adequate zeroth-order treatment for many

Table 2 The tops of the valence bands (VBs) and the bottoms of the conduction bands (CBs) of the defect-free (100) surface in the ground electronic state, and the highest occupied molecular orbitals (HOMOs) and the lowest unoccupied molecular orbitals (LUMOs) of the defect-containing (100) surface in the relaxed excited electronic state. The energies are calculated at the CIS level and given in eV

Crystal	Defect-free surface ground electronic state		Defect-containing bulk and surface relaxed excited electronic state		
	VBs	CBs	Impurity	HOMOs	LUMOs
LiCl	−11.630	−0.049	Ga^{+}	−3.006	0.0498
			Au^{+}	−3.419	0.0223
			Ca^{2+}	−6.939	−2.271
			Sr^{2+} [a]	−7.463	−2.251

[a] Reproducible data that were identical to those in [1]

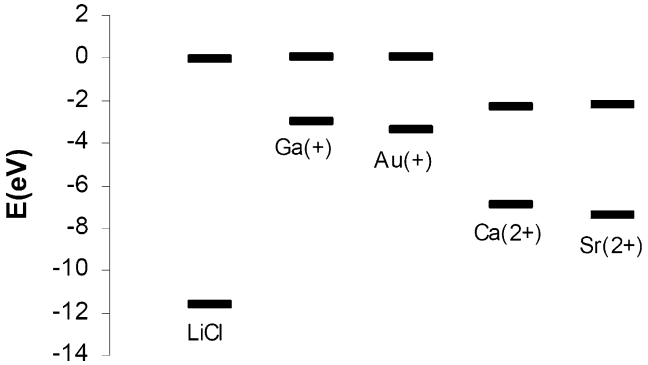

Fig. 3 Representation of the data in Table 2. The tops of the valence bands (VBs) and the bottoms of the conduction bands (CBs) of the defect-free (100) surface in the ground electronic state, and the highest occupied molecular orbitals (HOMOs) and the lowest unoccupied molecular orbitals (LUMOs) of the defect-containing (100) surface in the relaxed excited electronic state

excited states of molecules. Treatments of large molecular systems can be made practical by avoiding integral storage and transformation, and thus the configuration interaction singles method has a wide range of applicability. A satisfactory exploration of the potential energy surfaces and the accurate electronic properties of excited states can be achieved using an analytic configuration interaction singles gradient [21, 22]. This method includes some electron correlation in the excited states, but can provide reasonable accuracy for excitation energies in comparison with the simplest way of finding the lowest relaxed excited state in wide gap insulators—self-consistent field calculations of the triplet state [23]. Note that Sousa and Illas [24] have examined the impact that a proper electron correlation treatment could have on the optical absorption energy of F centers in MgO.

Compact effective potential basis sets

The Stevens, Basch, and Krauss compact effective potential (CEP) basis sets [25–27] were employed in the present calculations. In these CEP basis sets, double-zeta calculations are referred to as CEP-31 G and triple-zeta calculations as CEP-121 G. It should be noted that only one CEP basis set is defined beyond the second row, and the two basis sets are equivalent for these atoms. These basis sets have been used to calculate the equilibrium structures and spectroscopic properties of several molecules, and the results obtained compare extremely favorably with the corresponding all-electron calculations. The computations reported in this paper were carried out using the Gaussian 98 system [28].

Results and discussion

Stokes shifts

The configuration coordinate data for the F_{A1}:Ga^+, Au^+, Ca^{2+}, and Sr^{2+} laser color centers on the (100) surface of LiCl are given in Table 1, and the corresponding configuration coordinate curves are shown in Fig. 2. The strength of electron–phonon coupling as reflected by the value of the Stokes shift between the ground state and the low-lying excited state suggests that laser light generation is sensitive to the size of the impurity cation. Greater Stokes shifts are assigned to smaller cationic radii as follows: F_{A1}:Ga^+ is greater than F_{A1}:Au^+, and F_{A1}:Ca^{2+} is greater than F_{A1}:Sr^{2+}. This is in agreement with the values of $(Q_2 - Q_1)$. In addition, the smallest Stokes shift is assigned to the Au^+ ion, which has the largest electronegativity value and the smallest cationic size. Moreover, the Stokes shifts assigned to Ga^+ and Ca^{2+} as well as those assigned to Au^+ and Sr^{2+} are very similar, implying that (1) the potential of Ga^+ for laser light generation is similar to that of Ca^{2+}, and ditto for Au^+ and Sr^{2+}, and (2) sites with Ga^+ and Ca^{2+} are more laser active than those with Au^+ and Sr^{2+} based on the magnitude of each Stokes shift.

Optical–optical conversion

With a small Stokes shift, the optical–optical conversion efficiency will be enhanced. On the other hand, the reabsorption of emitted light by other F_A centers will also

Table 3 Energy barriers to the orientional destruction of the F_A^+ center on the (100) surface of LiCl due to the migration of the bulk anion to the assumed saddle-point ion configuration. The energies are calculated at the CIS level

Crystal	Impurity	Total energy of the original RES ion configuration (E_h)	Total energy of the saddle point ion configuration (E_h)	Energy barrier (E_h)	Energy barrier (eV)
LiCl	Ga^+	−473.568353859	−473.401667058	0.167	4.536
	Au^+	−351.567017457	−351.432625826	0.134	3.657
	Ca^{2+}	−216.879914144	−216.759194681	0.121	3.285
	Sr^{2+} [a]	−216.772094132	−216.611434261	0.161	4.372

[a] Reproducible data that were identical to those in [1]

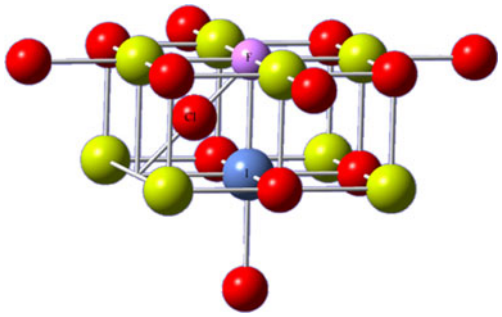

Fig. 4 Representation of the assumed relaxed excited-state saddle-point ion configuration responsible for the orientational destruction of the F_A center in the laser experiment. *Red* Cl^-, *yellow* Li^+, *pink (F)* F center, *blue (I)* impurity cation

increase. If the negative effect of reabsorption is stronger than the positive effect due to the conversion efficiency, then the laser activity decrease. Inspecting Table 1 reveals that the negative effect of reabsorption is expected to be stronger than the positive effect of a smaller cationic radius.

A laser-suitable defect should have relaxed excited states deep below the conduction band of the perfect crystal [11–13]. To examine this issue, we consider the band structure of the LiCl surface (i.e., the positions of the one-electron defect levels with respect to the perfect surface bands). In Table 2 and Fig. 3, we present the tops of the valence bands and the bottoms of the conduction bands for the ground states of the defect-free surfaces, as well as the highest occupied molecular orbitals and the lowest unoccupied molecular orbitals for the relaxed excited states of the defect-containing surfaces. As shown in Table 2 and Fig. 3, the excited states are below the lower edges of the conduction bands of the defect-free surfaces, implying that all of the present color centers are laser-suitable defects.

Orientational destruction

One consequence of the relaxed excited-state saddle-point ion configuration of the F_A center is a temperature-independent ionic reorientation during the pump cycle; i.e., a change of the center axis to a perpendicular (equivalent) orientation. After the emission process, the assumed saddle-point ion has a 50% chance of hopping to the <110> anion vacancy site opposite its starting location. Therefore, if the F_A center system is excited in either one of its absorption bands by polarized light with a direction of propagation parallel to the <100> axis and its electric field vector E parallel to the perpendicular <100> axis, the F_A centers excited by this E vector will quickly be reoriented to the <100> direction, at which point the F_A centers will no longer be excited, and this reoriented system will become experimentally transparent for the excitation light [5–8]. However, it has been observed experimentally and theoretically by many workers that no spectral region in the absorption range of the F_A band is completely transparent, even after prolonged preferential optical excitation of the F_A centers.

To theoretically examine the relaxed excited-state orientational destruction of the F_A center, we calculated the total energies of the original relaxed excited-state ion configuration and the assumed saddle-point ion configurations of the present color centers on the (100) surface of LiCl. The differences between the energies of these configurations (the energy barriers to orientational bleaching in a laser experiment) are given in Table 3 and are shown in Fig. 4. There is no clear dependence of the energy barrier on the cationic radius of the dopant. However, it is clear from the data in Table 3 that the value of the energy barrier due to the migration of the anion species to the vacancy site in the case of Ga^+ is very similar to that seen for Sr^{2+}, and the difference in the energy barriers for Au^+ and Ca^{2+} (3.657 − 3.285 eV) is only 0.38 eV. In other words, orientational destruction is generally probable for this type of F_A centers, particularly F_{A1}:Ca^{2+}, which has the highest reported Stokes shift. Experimentally, in order to avoid orientational bleaching, the pump polarization and the direction of propagation of the pump beam inside the crystal must be chosen such that they are not parallel to the <100> direction.

Optical memories

It is possible to use the reorientation of a defect such as an F_A center under the action of polarized light to store information [9, 10]. F_A centers can easily reorient at relatively low temperatures, and the reorientation efficiency is

Table 4 F_A^+ band gap E^+_{FA} and exciton band E_X on the (100) surface of LiCl. The energies are calculated at the DFT level

Crystal	Impurity	CB (E_h)	VB (E_h)	E^+_{FA} (E_h)	E^+_{FA} (eV)	E_{normal} (E_h)	$E_{exciton}$ (E_h)	E_X (E_h)	E_X (eV)	$E_X - E^+_{FA}$ (eV)
LiCl	Ga^+	−0.086	−0.054	−0.032	−0.866	−478.214	−477.723	0.491	13.366	12.875
	Au^+	−0.100	−0.057	−0.043	−1.182	−355.950	−355.459	0.492	13.380	12.888
	Ca^{2+}	−0.252	−0.139	−0.113	−3.079	−220.417	−219.954	0.463	12.610	12.147
	Sr^{2+a}	−0.252	−0.138	−0.114	−3.109	−220.329	−219.863	0.465	12.664	12.199

[a] Reproducible data that were identical to those in [1]

$E^+_{FA} = CB - VB, E_X = E_{exciton} - E_{normal}$

very high above 140 K, which implies high recording sensitivity. However, at 55 K, this efficiency practically vanishes; thus, it is possible to "read" with polarized light. In the dark, there is no thermal reorientation of the centers, and thus the information may be stored indefinitely. As shown in Table 3, the reorientation efficiency (probability) of F_A centers due to the migration of the bulk anions to the assumed saddle-point ion configuration increases as the size of the impurity cation increases from Ga^+ to Au^+ and from Ca^{2+} to Sr^{2+}. This implies a high recording sensitivity for F_{A1}:Ga^+ relative to F_{A1}:Au^+, and for F_{A1}:Ca^{2+} relative to F_{A1}:Sr^{2+}. Indeed, the highest recording sensitivity is assigned to F_{A1}:Ga^+, as it has the largest energy barrier.

Glasner–Tompkins relation

Glasner and Tompkins [29] reported an empirical relationship between the principal optical absorption of F centers in solids and the fundamental absorption of the host crystal. The difference between the first exciton absorption energy E_X and the F-band energy E_F was found to depend almost exclusively on the negative ion species. In other words, the Glasner–Tompkins empirical rule suggests that the energy difference between the fundamental absorption of an alkali halide and the F band is very nearly only a function of the halide species. Exciton band E_X, F-band E_F, $(E_X - E_F)$ and $<(E_X - E_F)>$ values for twelve alkali halides have been reported by Malghani and Smith [30] and for LiH and LiF by Shalabi et al. [31]. The dependence of the Glasner–Tompkins relation on the impurity cation and the surface coordination number (flat, edge and corner) has also been reported for MgO, KCl and AgBr by Shalabi et al. [11, 32]. However, no attempt has been made to clarify the dependence of the Glasner–Tompkins relation on the size of the impurity cation on the (100) surface of LiCl.

To apply the Glasner–Tompkins relation to the present F_A centers, we have to calculate the corresponding band gaps and exciton bands. A complete treatment of the host dependence of the band gaps would involve theories of excitons and defects [33–40] that take into account the band structure. Since this would be a major undertaking and well beyond our present goal, we used the simple electron transfer model of the fundamental optical absorption of ionic solids developed by Hilsch and Pohl [41]. This model, in its simplest form, explains the fundamental optical absorption EX as the transfer of an electron from a negative ion to a neighboring positive ion, both positioned adjacent to the defect site. It seems likely that all color centers have perturbed excitons that form nearby. We therefore calculated EX as the change in Coulomb energy associated with the transfer of an electron from a halide anion to a lithium cation, both of which are located adjacent to the F_A center, and calculated E_{FA} as the energy difference between the highest occupied molecular orbital and the lowest unoccupied molecular orbital energy levels. The correlation between the surface ion coordination, the F_A center, and the energy difference between the exciton band E_X and the band gap E_{FA} is given in Table 4. The results shown in the table confirm that while the energy difference between the exciton band E_X and band gap E_{FA} is directly proportional to the radius of the dopant cation, it is inversely proportional to the electronegativity, F_{A1}:Au^+ > Ga^+ > Sr^{2+} > Ca^{2+}. This suggests that the difference between the first exciton absorption energy E_X and the F-band energy E_F depends on not only the anion species but also the size and electronegativity of the cation species.

Conclusions

The value of the Stokes shift between the ground state and the low-lying excited state suggests that laser light generation is sensitive to the size of the impurity cation. Greater Stokes shifts are assigned to smaller cationic radii as follows: F_{A1}:Ga^+ is greater than that of F_{A1}:Au^+, and F_{A1}:Ca^{2+} is greater than that of F_{A1}:Sr^{2+}. Moreover, the Stokes shifts assigned to Ga^+ and Ca^{2+} are very similar, and those assigned to Au^+ and Sr^{2+} are nearly identical . An examination of the band structure of the LiCl surface (i.e., the positions of the one-electron defect levels with respect to the perfect surface bands) showed that the excited states are below the lower edges of the conduction bands of the defect-free surfaces, implying that all of the color centers considered in this work are laser-suitable defects. Calculations of the total energies of the original relaxed excited-state ion configuration and the assumed saddle-point ion configuration of each center suggest that the energy barrier to the migration of the anion species to the vacancy site in the case of Ga^+ is very similar in size to that of Sr^{2+}, and the difference in the energy barriers of Au^+ and Ca^{2+} is only 0.38 eV. Calculations of the Glasner–Tompkins relation for the present F_A centers indicated that the difference between the first exciton absorption energy E_X and the F-band energy E_F depends not only on the negative ion species but also on the size of the impurity cation.

References

1. Abdel-Aal S (2007) Artificial polarization effects on F_{A1}:Sr^{2+} laser and coadsorption of CN and O at LiCl (001) surface: first principles calculations. J Mol Struct (THEOCHEM) 816:85–96
2. Joshi RV, Kekan NL (1980) Effect of activator content on the thermoluminescence of pretreated NaCl: Sr. Radiat Eff Lett 57:135–136

3. Greneche JM, Venkatesan M, Suryanarayanam R, Coey JMD (2001) Mössbauer spectrometry of A_2FeMoO_6 (A = Ca, Sr, Ba): search for antiphase domains. Phys Rev B 63:174403–174407
4. Fowler WB (1986) Physics of color centers. Academic, New York
5. Gellermann W, Luty F, Pollock CR (1981) Optical properties and stable, broadly tunable cw laser operation of new FA-centers in Tl^+-doped alkali-halides. Opt Commun 39:391–395
6. Gellermann W, Jock T, Luty F (1984) In: Abstracts of the International Conference on Defects in Insulating Crystals, Salt Lake City, UT, USA, 20–24 Aug 1984, pp 167 (unpublished)
7. Glaus S, Calzaferri G, Hoffmann R (2002) Electronic properties of the silver–silver chloride cluster interface. Chem Eur J 8:1785–1794
8. Glaus S, Calzaferri G (2003) The band structures of the silver halides AgF, AgCl, and AgBr: a comparative study. Photochem Photobiol Sci 2:398–401
9. Fitchen DB (1968) Chapter 5. In: Fowler WB (ed) Physics of color centers. Academic, New York
10. Gellermann W (1991) Color center lasers. J Phys Chem Solids 52:249–297
11. Shalabi AS, El-Essawy TF, Assem MM, Abdel-Aal S (2002) $F_A(Ga^+, In^+, Tl^+)$ tunable laser activity and interaction of halogen atoms (F, Cl, Br, I, At) at the (001) surface of KCl crystal: ab initio calculations. Curr Appl Phys 2:97–105
12. Shalabi AS (2002) F^+ tunable laser activity and interaction of atomic halogens (F, Cl and Br) at the low coordinated surface sites of SrO: ab initio and DFT calculations. J Mol Model 8:314–326
13. Shalabi AS, Alansari IAZ, Al-Naimi KKh, Kamel MA, El-Mahdy AM, Taha HO, Shalaby MM (2004) The role of F_A:K^+ and F_A:Na^+ defects in laser light generation and color image formation at the (100) and (110) surface sites of AgCl and AgBr: first principles calculations. Phys Chem Chem Phys 6:626–636
14. Colbourn EA (1999) In: Catlow CRA (ed) Advances in solid state chemistry, vol I. JAI, London
15. Shalabi AS, El-Mahdy AM, Kamel MA, Ammar HY (2000) Excitons, electron center diffusion and adsorptivity of atomic H on LiH (001) surface: ab initio study. Physica B 292:59–70
16. Shalabi AS, El-Mahdy AM, Kamel MA, Ismail GH (2001) STH centers in LiF and NaH crystals: ab initio calculations. J Phys Chem Solids 60:1007–1013
17. Shalabi AS, El-Mahdy AM (1999) An ab initio approach to bulk and surface properties of many-body energies and adsorptivity in MgO crystal. J Phys Chem Solids 60:305–315
18. Shalabi AS, El-Mahdy AM (2001) Adsorptivity of atomic H and coadsorptivity of Mg and O ions on regular and irregular surfaces of MgO: DFT calculations. Phys Lett A 281:176–186
19. Ferrari AM, Xiao C, Neyman KM, Pacchioni G, Rosch N (1999) Pd and Ag dimers and tetramers adsorbed at the MgO(001) surface: a density functional study. Phys Chem Chem Phys 1:4655–4661
20. Fowler WB, Dexter DL (1965) Detailed balance in optical transitions in molecules and solids. Chem Phys 43:1768–1772
21. Foresman JB, Head-Gordon M, Pople JA, Frisch MJ (1992) Toward a systematic molecular orbital theory for excited states. J Phys Chem 96:135–149
22. Foresman JB (1996) Exploring chemistry with electronic structure methods, 2nd edn. Gaussian Inc., Pittsburgh
23. Shluger AL, Sushko PV, Kantorovich LN (1999) Spectroscopy of low-coordinated surface sites: theoretical study of MgO. Phys Rev B 59:2417–2430
24. Sousa C, Illas F (2001) On the accurate prediction of the optical absorption energy of F-centers in MgO from explicitly correlated ab initio cluster model calculations. J Chem Phys 115:1435–1439
25. Stevens W, Basch H, Krauss J (1984) Compact effective potentials and efficient shared–exponent basis sets for the first– and second–row atoms. J Chem Phys 81:6026–6033
26. Stevens W, Krauss M, Basch H, Jasien PG (1992) Relativistic compact effective potentials and efficient, shared-exponent basis sets for the third-, fourth-, and fifth-row atoms. Can J Chem 70:612–630
27. Cundari TR, Stevens WJ (1993) Effective core potential methods for the lanthanides. J Chem Phys 98:5555–5565
28. Frisch MJ, Trucks GW, Schlegel HB et al (1998) Gaussian 98, revision A6. Gaussian Inc., Pittsburgh
29. Glasner A, Tompkins FC (1953) Note on some regularities of the absorption band maxima of colored alkali metal halides. J Chem Phys 21:1817–1818
30. Malghani MS, Smith DY (1991) The physical basis of the Glasner–Tompkins relations between F-center and exciton spectra. Bull Am Phys Soc 36:1681
31. Shalabi AS, El-Mahdy AM, Eid Kh M, Kamel MA, El-Barbary AA (1999) Glasner–Tompkins relation and reorientation of U centers in LiF crystals. Phys Rev B 60:9377–9382
32. Shalabi AS, El-Essawy TF, Assem MM, Abdel-Aal S (2002) F_2^+ laser activity and photographic sensitization at the low coordinated surfaces of AgBr: ab initio calculations. Physica B 315:13–28
33. Plekhanov VG (1996) Isotope-induced energy-spectrum renormalization of the Wannier–Mott exciton in LiH crystals. Phys Rev B 54:3869–3877
34. Connel-Bronin AAO (1996) Mechanism of resonant Rayleigh scattering of polaritons in diffuse reflection spectra of LiH crystals. Phys Stat Sol B 38:1489–1491
35. Koster GF, Slater JC (1954) (1954) Wave functions for impurity levels. Phys Rev 95:1167–1176
36. Koster GF, Slater JC (1954) Simplified impurity calculation. Phys Rev 96:1208–1223
37. Crawford JH, Slifkin LM (eds) (1972) Point defects in solids. Plenum, New York
38. Hayes W, Stoneham AA (1985) Defects and defect processes in non-metallic solids. Wiley, New York
39. Kotomin E, Popov A (1998) Radiation-induced point defects in simple oxides. Nucl Instrum Methods B 141:1–15 (and references therein)
40. Knox RS (1963) Theory of excitons. Academic, New York
41. Hilsch R, Pohl RW (1929) Einige dispersionsfrequenzen der alkalihalogenidkristalle im achumanngebiet. Z Phys 59:812–819